Pergamon

Electrochimica Acta, Vol. 42, No. 9, pp. 1427–1434, 1997

PII: S0013-4686(96)00366-0
0013-4686/97 $17.00 + 0.00

Synergistic inhibition in low chloride media

G. Gunasekaran,[a] N. Palanisamy,[a] B. V. Appa Rao[b] and V. S. Muralidharan[a]**

[a]Central Electrochemical Research Institute, Karaikudi, Tamil Nadu India [b]Department of Chemistry, Regional Engineering College, Warangal, Andhra Pradesh, India

(Received 12 June 1996)

Abstract—Electrochemical and weight change methods were used to study the synergistic inhibition offered by Zn^{2+} ions and 2 carboxyethyl phosphonic acid (2CEPA) to the corrosion of mild steel in 60 ppm chloride solutions. The surface film was found to contain $Zn(OH)_2$ along with iron phosphonate complex. The diffusion of iron, phosphonate complex and H^+ ions through this film determines the dissolution rate of iron. © 1997 Published by Elsevier Science Ltd. All rights reserved.

Key words: Synergistic inhibition, 2 carboxy ethyl phosphonic acid, XRD, FT-IR, ESCA, *uv*-luminescence and *uv*-diffused reflectance spectra.

INTRODUCTION

The corrosion inhibition of steel in neutral oxygen saturated environments is mainly decided by the ability of the complexing ions to form insoluble complex with metal ions existing in the solution, which precipitate on the surface to form a three-dimensional protective layer. Phosphonic acids at low concentrations favoured inhibition by repairing the pores of the oxide layer, while at higher concentrations the dissolution of the oxide is favoured. Zn^{2+} ions at lower concentrations were less effective in offering inhibition in the presence of HEDP (hydroxy ethylidene 1,1-diphosphonic acid) while at 10^{-2} M they offered enhanced inhibition. The presence of Ca^{2+} and Zn^{2+} ions enhanced the inhibition offered by phosphonates [1–8].

The present work aims to understand the mechanism of synergism offered by Zn^{2+} ions in the presence of 2-carboxy ethyl phosphonic acids (2CEPA) for the corrosion of mild steel in 60 ppm chloride solutions, a situation commonly encountered in cooling water technology.

The present study was carried out to understand whether (a) zinc forms a complex with phosphonic acid and offers enhanced protection; or (b) zinc catalyses the formation of iron–phosphonate complex; or (c) zinc stabilizes the formation of iron oxide film by closing the pores with $Zn(OH)_2$.

*Author to whom correspondence should be addressed.

EXPERIMENTAL

Preparation of the specimens

Mild steel (0.02–0.3% S, 0.3–0.8% P, 0.4–0.5% Mn, 0.1–0.2% C and the rest Fe) was used. Specimens of dimensions 1 × 4 × 0.2 cm were used for weight loss and surface examination studies. Electrochemical measurements were carried out on 0.5 cm dia circular electrodes. The steel surfaces were polished successively in 1/0 to 4/0 emery papers and degreased with trichloro ethylene.

Weight change measurements

Mild steel specimens in triplicate were immersed in 100 ml of the test solutions for a period of 7 days. The changes in weight were followed to an accuracy of ±5%. The percentage inhibition efficiency = $[(W_1 - W_2)/W_1] \times 100$ where W_1 and W_2 are weight losses of steel in uninhibited and inhibited chloride solutions.

Electrochemical measurements

A three-electrode cell assembly was used. The mild steel specimens were used as the working electrode, large platinum foil as counter electrode and saturated calomel electrode as reference electrode, respectively. The polarization studies were carried out using EG&G PAR model 173/Potentiostat in combination with model 175 universal programmer and Rikadenki *x–y* recorder.

Examination of surface films

The polished mild steel specimens were completely immersed in 60 ppm chloride solutions with and without inhibitors. After a specified time interval, the specimens were taken out and washed with distilled water and dried. The dried specimens and the solutions were used for spectral analysis.

The X-ray diffraction studies were carried out on the surface films formed under various test conditions using a computer-controlled X-ray powder diffractometer (JOEL 8030) with Cu-K_γ (Ni filtered) radiation (λ = 1.5418 Å) at a rating of 40 kV, 20 mA. The scan rate was 0.05°–20° per step and the measuring time was one second per step.

uv-Visible diffused reflectance spectra of the films formed on the metal were recorded using a Hitachi-U3400 Spectrophotometer.

uv-Luminescence emission spectra of the film were recorded using a Hitachi 650-10S fluorescence spectrophotometer equipped with a 150 W xenon lamp and Hamamatsu K 929 F photomultiplier tube. The emission spectra were corrected for the spectral response of the photomultiplier tube.

X-ray photo electron spectroscopic (ESCA) analysis was made on the films formed on the metal.

The surface film formed on mild steel was scratched carefully and the powder obtained was thoroughly mixed so as to make it uniform. FTIR spectrum of the powder (KBr pellet) was recorded using a Perkin–Elmer 1600 FTIR spectrophotometer.

Preparation of the metal complexes

Analar grade chemicals were used. 2-carboxy ethyl phosphonic acid (2CEPA) supplied by Aldrich, U.S.A., was used. The zinc-2CEPA complex was precipitated from dilute $ZnSO_4$ solution added to sodium salt of 2CEPA solution maintained at pH 7. The precipitate was washed and dried. The ferric-2CEPA complex was precipitated when dilute neutral $FeCl_3$ solution was added to 2CEPA solution maintained at pH 7. The precipitate was washed and dried.

RESULTS

Weight change measurements

The corrosion of steel in 60 ppm Cl^- solutions was enhanced in the presence of 2CEPA. Corrosion inhibition was observed only above 50 ppm each of Zn^{2+} ions and 2CEPA (Fig. 1).

Inhibition efficiency was above 80% in the presence of 50 ppm Zn^{2+} ions. The decrease of inhibition efficiency with temperature suggests the film formed on the surface dissolves (Fig. 2).

The introduction of Zn^{2+} ions increased the corrosion current density by nearly 3 times, while 100 ppm of 2CEPA doubled it (Fig. 3). The anodic Tafel slopes increased in the presence of Zn^{2+} ions and 2CEPA. In the presence of Zn^{2+} ions and 2CEPA, the corrosion current density decreased (Table 1). A decrease of pH increased the corrosion current density without influencing the anodic Tafel slope, suggesting the chemical dissolution of the inhibitor film with pH decreases (Table 2).

Surface film characterization

XRD patterns of the surface film (Fig. 4) revealed that the surface obtained after immersion in 60 ppm Cl^- solutions [curve A] exhibited predominant peaks at 2θ = 42, 63 and 83° with intensities of 302, 253 and 279 CPS, respectively. The surface obtained from the Cl^- solutions containing Zn^{2+} ions, 2CEPA solutions containing chloride ions (curves B and C) exhibited similar behaviour. The curve D corresponds to the surface film dipped in Cl^- solutions containing both Zn^{2+} ions and 2CEPA. Predominantly peaks at 42, 63

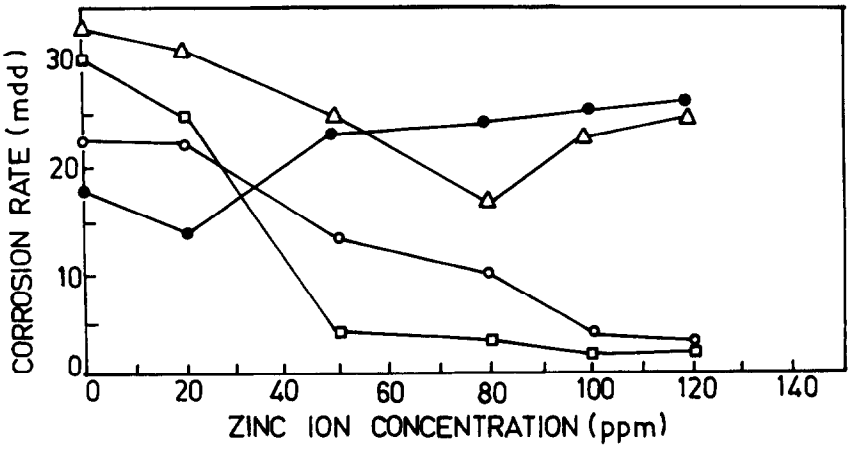

Fig. 1. Variation of corrosion rate with various zinc concentrations in 60 ppm Cl^- solutions at pH 7 at 30 C. Synergistic influence of 2CEPA. (●) No 2CEPA; (△) 20 ppm 2CEPA; (○) 50 ppm 2CEPA; and (□) 100 ppm 2CEPA.

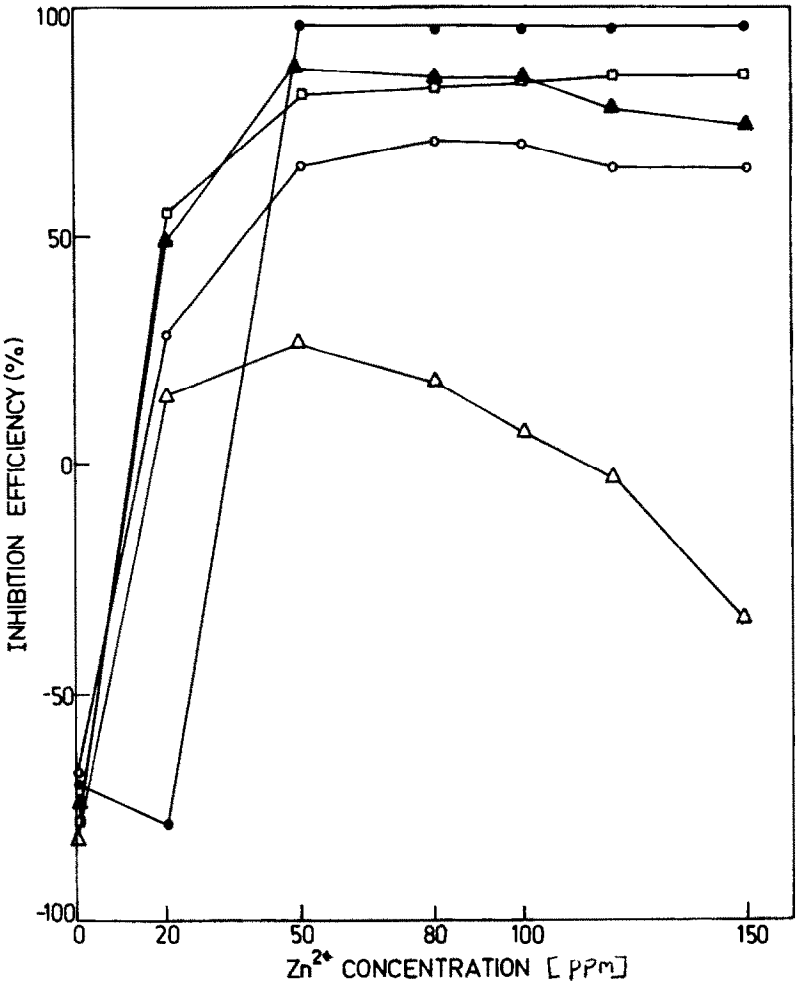

Fig. 2. Variation of the percentage inhibition efficiency with various Zn^{2+} concentrations in 60 ppm chloride solutions containing 100 ppm 2CEPA at pH 7. Effect of temperature. (●) 30°C; (□) 50°C; (▲) 60°C; (○) 70°C; and (△) 80°C.

and 83° with intensities of 612, 283 and 332 CPS were seen. These intensities are much higher compared to those in curve A.

The peaks obtained at $2\theta = 35$ and 42° revealed the presence of Fe_3O_4 and peaks at 30 and 63° suggest the formation of ν-FeOOH.

uv-Reflectance spectra (Fig. 5) of the surface ligand in Zn^{2+} ions and 2CEPA solutions revealed a wavelength transition of 550 nm, indicating iron oxide. The surface dipped in solution containing both the species indicated not only the absence of iron oxide but an appearance of a new peak at 290 nm. In order to identify this peak, *uv*-visible absorption spectra of the solution was obtained (Fig. 6). The 2CEPA solution exhibited a peak at 190 nm. This peak broadening appeared in the solution containing Zn^{2+} ions and 2CEPA suggesting the formation of zinc complex in solution. At the end of 7 days of immersion of mild steel, the solution containing Zn^{2+} ions and 2CEPA exhibited a large peak at 190 nm, along with a peak at 290 nm suggesting the formation of iron phosphonate complex in solution. In order to confirm the presence of iron phosphonate complex fresh solutions of Fe^{3+} ions and 2CEPA were prepared and their spectra exhibited a peak at 290 nm. *uv*-Luminescence emission spectra (Fig. 7) of different solutions were taken. The solution of 2CEPA (curve A) exhibited a peak at 465 nm. Mild steel specimens were kept for 7 days in 60 ppm Cl^- solutions containing 100 ppm 2CEPA. This solution spectra (curve B) also exhibited a peak at 465 nm. After 7 days of immersion of mild steel the solution containing both Zn^{2+} ions and 2CEPA was analysed and its spectra (curve C) exhibited an additional peak at 445 nm. In order to confirm that this peak at 445 nm is due to iron phosphonate complex, fresh solutions of $FeCl_3$ containing 2CEPA were prepared and the solution spectra exhibited a peak at 445 nm, confirming the presence of iron phosphonate complex in solution [9, 10]. The peak which appeared at 465 nm in 2CEPA solutions may be due to the presence of alkali metal ion-2CEPA complexes.

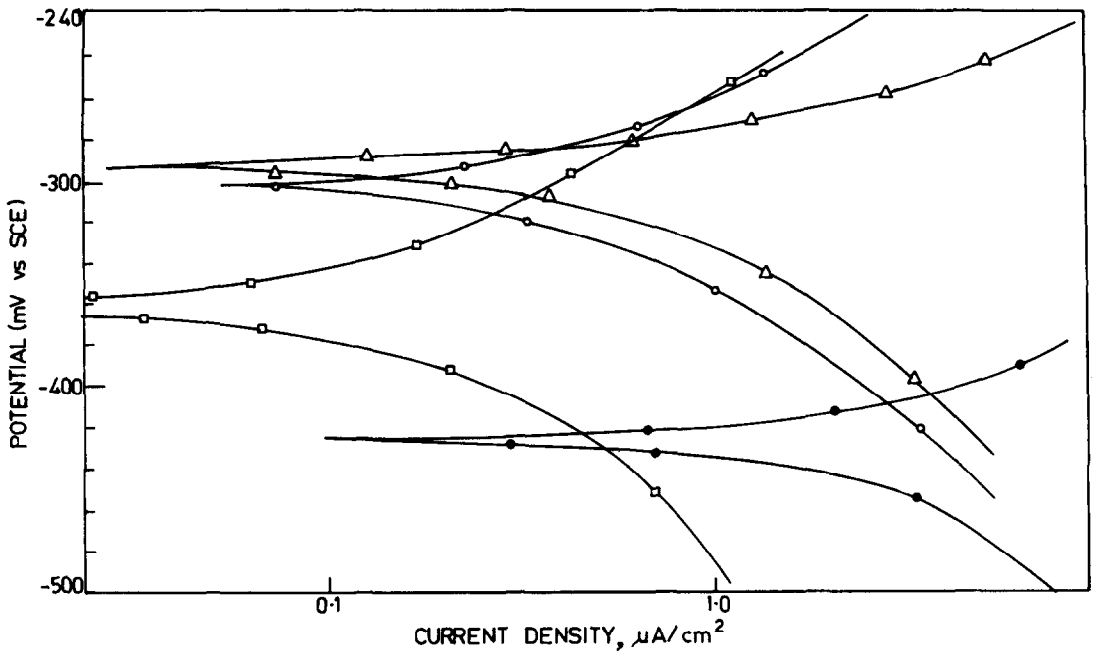

Fig. 3. E–log i polarization curves for the corrosion of mild steel in 60 ppm chloride solutions, pH 7 at 30°C. (△) Blank; (●) + 100 ppm Zn^{2+}; (○) + 100 ppm 2CEPA; and (□) + 100 ppm Zn^{2+} + 100 ppm 2CEPA.

The *uv*-luminescence emission spectra of the solid 2CEPA, iron complex and zinc complex (Fig. 8) excited at 404 nm were obtained. The solid 2CEPA spectra did not exhibit any peak. The zinc complex exhibited a peak of 465 nm and iron complex at 445 nm. The surface films obtained after immersing steel in the solutions of 2CEPA, Zn^{2+} ions and Zn^{2+} + 2CEPA were excited at 404 nm (Fig. 9). The emission spectra obtained on the film kept in Zn^{2+} + 2CEPA solution exhibited a peak at 445 nm suggesting the complex formation on the surface is iron phosphonate complex and not zinc complex.

In order to confirm the presence of iron complex, FTIR spectra of the surface film obtained from Zn^{2+} + 2CEPA was obtained (Fig. 10). The spectra of the iron-2CEPA complex was obtained for comparison with the band for the C=O group in the complex formation. The stretching vibration frequency of the phosphonyl group (—P=O) gave a band at 1100 cm^{-1} and 912 cm^{-1} [10]. The presence of $Zn(OH)_2$ was also indicated by a band at 1320 cm^{-1}.

The ESCA pattern of the protective film formed on mild steel surface in Zn^{2+}-2CEPA system is shown in Fig. 11. The peaks at 13 eV (3 S 1/2), 134 eV (2 P 1/2) and 191 eV (2 S 1/2) revealed the presence of phosphorous atom. The peak at 134 eV was due to P in phosphorous acid (—PO_3H_2 or P^{5+}). Peaks of zinc were exhibited at 94 eV (2 S 1/2), 140 eV (3 S 1/2) and 1022 eV (2 P 3/2). The peaks at 92 eV (3 P 1/2) and

Table 1.
Parameters obtained from polarization curves in 60 ppm chloride solutions at pH 7 at 30°C

System	E_{corr} vs *sce* (mV)	Tafel slopes (±10 mV decade)		Corrosion current density (μA cm^2 (±0.1))	
		Anodic	Cathodic	Anodic	Cathodic
Blank	−294	54	110	6	6
100 ppm + 2CEPA	−298	80	84	12	12
100 ppm − Zn^{2+} ions	−426	84	130	20	20
100 ppm + 2CEPA + 100 ppm Zn^{2+}	−362	88	86	0.1	0.1

Table 2.
Parameters derived from polarization curves in 60 ppm Cl^- + 100 ppm 2CEPA + 100 ppm Zn^{2+} solution, the effect of pH

pH	E_{corr} vs *sce* (mV)	Tafel slopes (±10 mV decade) Anodic	Tafel slopes (±10 mV decade) Cathodic	Corrosion current density (μA cm^2 (±0.1)) Anodic	Corrosion current density (μA cm^2 (±0.1)) Cathodic
7	−362	88	86	0.1	0.1
5	−544	76	132	1.5	1.5
3	−547	77	140	4.7	4.7

721 eV (2 P 1/2) are mainly due to the presence of Fe^{2+} and Fe^{3+} ions. The peaks at 290 eV, 293 eV and 296 eV are mainly due to the presence of C—C, C—O and C=O groups. A peak at 201 eV is due to Cl^- ion. The observed peak at 534 eV is due to oxygen (1 S 1/2) in phosphonic acid attached to the iron atom. This reveals that the oxygen in phosphonic acid is bonded with the iron atom. These suggest that the inhibitive film consists of iron phosphonate complex in the presence of Zn^{2+} ions.

DISCUSSION

Mechanism of dissolution

The composition and the structure of the films formed on iron remains the subject of continued interest [11]. The dissolution occurs as

$$Fe + H_2O \leftrightarrow FeOH_{ads} + e + H^+,$$

$$FeOH_{ads} \leftrightarrow FeOH^+ + e,$$

$$FeOH^+ \leftrightarrow Fe^{2+} + OH^-.$$

In chloride solutions, the formation of the chloro complex is as follows:

$$Fe^{2+} + mH_2O + nCl^- \leftrightarrow Fe(OH)_m(Cl)_n^{2-n-m} + mH^+,$$

where m varies from 1.7 to 1.6; $n = 0.3$ to 0.2.

On iron, various oxhydroxy chloro complexes with a general formula $Fe_3(OH)_5Cl$ or $Fe_6(OH)_{11}Cl$ are known in Cl^- solutions; prolonged exposure resulted in $3Fe(OH)_2 \cdot Fe(OH)Cl \cdot n\ H_2O$ [12].

Synergistic inhibition

Synergism is defined as the reinforcement of inhibitive action of a compound, usually employed in

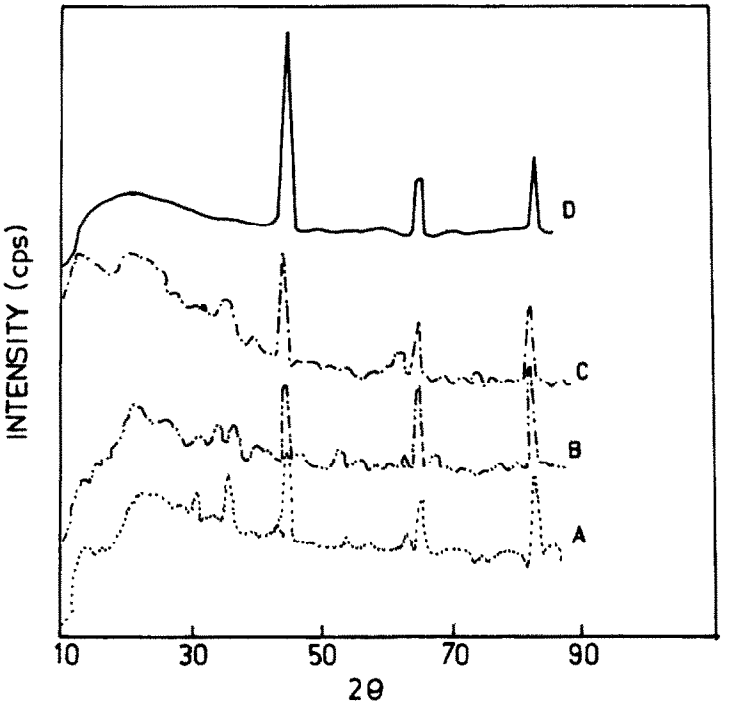

Fig. 4. XRD pattern obtained on the surface film formed on mild steel at the end of 3 days in different solutions at pH 7. Curve (A) 60 ppm chloride; (B) 100 ppm 2CEPA; (C) 100 ppm Zn^{2+}; and (D) 100 ppm 2CEPA + 100 ppm Zn^{2+}.

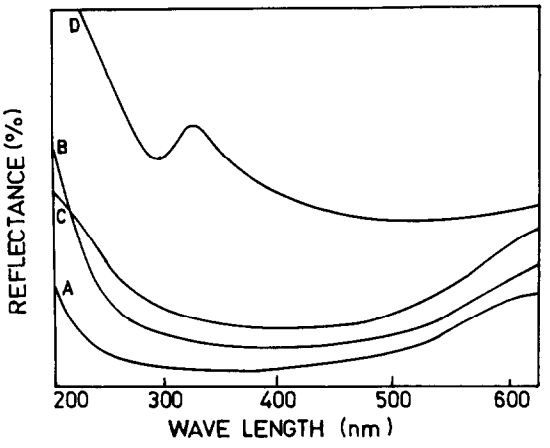

Fig. 5. *uv*-Reflectance spectra of the surface film formed on mild steel at the end of 3 days in different solutions at pH 7. Curve (A) 60 ppm chloride; (B) 100 ppm 2CEPA; (C) 100 ppm Zn^{2+}; and (D) 100 ppm Zn^{2+} + 100 ppm 2CEPA.

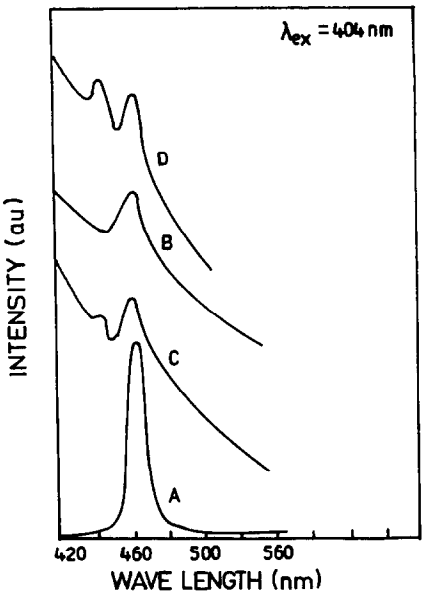

Fig. 7. *uv*-Luminescence emission spectra of the solution containing various cations. Effect of exposure time of steel at λ_{ex} = 404 nm. Curve (A) 100 ppm 2CEPA; (B) 100 ppm 2CEPA (7 days); (C) 100 ppm Zn^{2+} + 100 ppm 2CEPA (7 days); and (D) 100 ppm Fe^{3+} + 100 ppm 2CEPA.

higher concentrations, by the addition of a small amount of a second compound, even though the second compound is less effective when used alone.

In acid media usually an amine with an anion exhibits synergism by adsorption.

Three different models, usually the overlap model, the co-adsorption model and the electrostatic co-adhesion model, have been proposed. The stabilization by adsorbed anionic layer by organic cations takes place by covalent bonding [13–17]. In neutral chloride solutions, HEDP offered inhibition only when the Zn^{2+} ions concentration was above 10^{-2} M. At lower concentrations of Zn^{2+} ions the inhibition is less. Dodecyl sodium phosphonate offered inhibition by forming an inhibitor double-layer. The first adsorbed layer was due to polar head

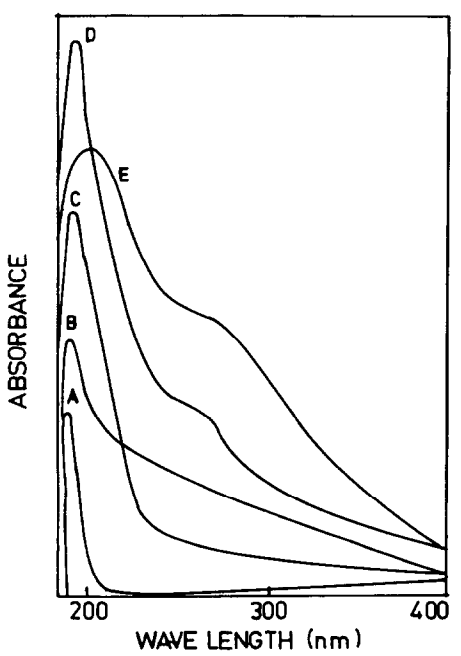

Fig. 6. *uv*-Absorbance spectra of the solution containing various cations in 60 ppm chloride solutions. Influence of exposure time of steel. Curve (A) 100 ppm 2CEPA (10 min); (B) 100 ppm 2CEPA (7 days); (C) 100 ppm Zn^{2+} + 100 ppm 2CEPA (2 days); (D) 100 ppm Zn^{2+} + 100 ppm 2CEPA (7 days); and (E) 100 ppm Fe^{3+} + 100 ppm 2CEPA (10 min).

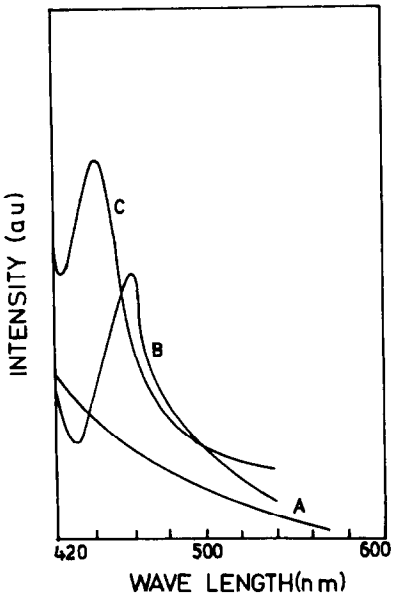

Fig. 8. *uv*-Luminescence spectra of solids at λ_{ex} = 404 nm. Curve (A) 2CEPA; (B) Zn-2CEPA complex; and (C) Fe(III)-2CEPA complex.

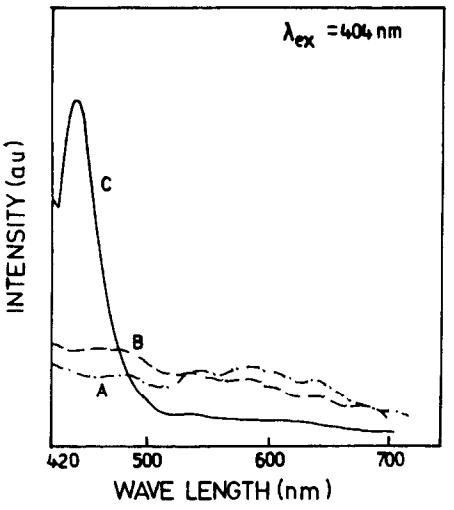

Fig. 9. *uv*-Luminescence emission spectra of the surface film formed on mild steel in 60 ppm chloride solutions at $\lambda_{ex} = 404$ nm. Curve (A) 100 ppm 2CEPA; (B) 100 ppm Zn^{2+} ions; and (C) 100 ppm Zn^{2+} + 100 ppm 2CEPA.

groups, and the second stabilized layer resulted from the hydrophobic character of the CH_2 group chain.

Earlier studies revealed that phosphonates at higher concentrations and zinc ions at lower concentrations favoured metal dissolution (*loc. cit.*). However, at critical concentrations of Zn^{2+} ions and phosphonic acids inhibition efficiencies of >80% were observed.

The enhanced production of $FeOH_{ads}$ and its subsequent conversion to $FeOH^{+}_{ads}$ favoured dissolution. The Zn^{2+} ions and 2CEPA anions reacted with $FeOH^{+}_{ads}$ and enhanced dissolution. On prolonged exposure, the surface chelation occurs as

$$FeOH + nX^{-} \rightarrow FeOHX_n$$

where X is 2CEPA ligand.

The anodic reaction order *wrt* 2CEPA at pH 7 was 0.8 ± 0.1 suggests that $n = 1$.

The presence of Zn^{2+} ions in the concentration range studied favoured the dissolution, and the anodic reaction order *wrt* Zn^{2+} ions at pH 7 was 1.2 ± 0.1.

$$FeOH^{+}_{ads} + Zn^{2+} \leftrightarrow ZnOH^{+} + Fe^{2+},$$

$$ZnOH^{+} + OH^{+} \rightarrow Zn(OH)_2.$$

FTIR studies on the surface inhibitor film confirmed this.

The overall dissolution reaction is determined by the diffusion of $FeOH^{+}$ and Fe^{2+} ions, H^{+} ions and Fe*x* away from the surface film. At steady-state, the Fe*x* and H^{+} produced much diffusion away continuously. The current is proportional to the diffusion rates of Fe*x* and H^{+} ions.

$$i_a = 2FD_{Fex}(da_{Fex}/dx)_{x \pm 0}$$

$$= 2F(D_{H^+}/m)(da_{H^+}/dx)_{x=0}.$$

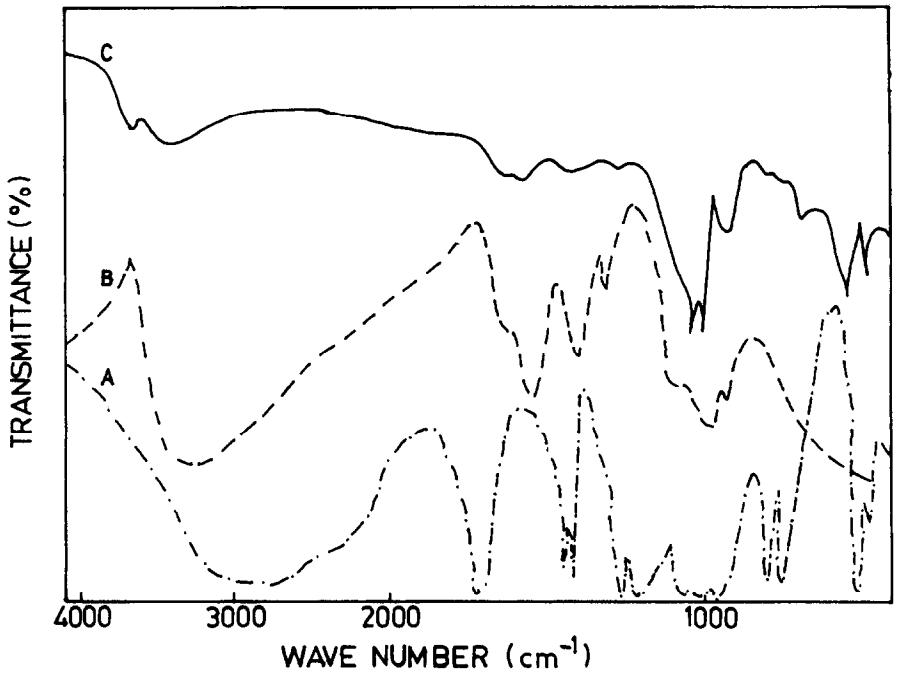

Fig. 10. FTIR spectra of the various solids and surface films formed on iron. Curve (A) 2CEPA solid; (B) Fe(III)-2CEPA (solid); and (C) surface film formed on steel in 60 ppm Cl^{-} solution containing 100 ppm Zn^{2+} + 100 ppm 2CEPA.

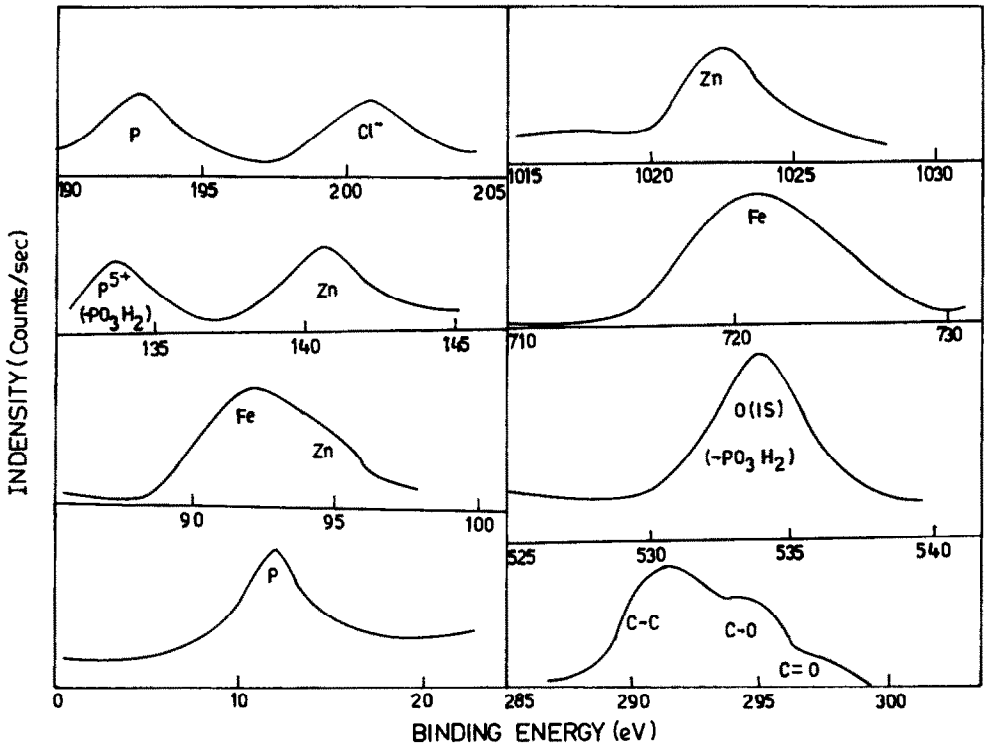

Fig. 11. ESCA (counts vs binding energy) of the surface film formed on mild steel immersed in 60 ppm chloride + 100 ppm Zn^{2+} + 100 ppm 2CEPA.

As the concentration of $(H^+)_{x=0} = 0$

$$i_a = 2F(D_{H^+}/m\delta)(a_{H^+})_{x=0}$$

$$= 2F(D_{Fe^{++}}/\delta)(da_{H^+}/dx)_{x=0}$$

where x is the film/solution interface and a is the thickness of the inhibitor film.

The observed anodic Tafel slope of 80 mV/decade in all solutions confirms this.

CONCLUSIONS

Zn^{2+} ions and 2CEPA offered inhibition to corrosion of steel in 60 ppm Cl^- solutions. The surface inhibitor film was found to contain $Zn(OH)_2$, Fe_2O_3 along with iron phosphonate complex. The dissolution of iron was controlled by the diffusion of iron phosphonate soluble complex and H^+ ions through this inhibitor film.

REFERENCES

1. E. Kalman, B. Varhegyi, I. Bako, I. Felhosi, F. H. Karman and A. Shabar, *J. Electrochem. Soc.* **14,** 3357 (1994).
2. A Veres, G. Reinhard and E. Kalman, *Brit. Corros. J.* **27,** 147 (1992).
3. F. H. Karman, E. Kalman, L. Varallyai and J. Konya, *Z. Naturforsch.* **469,** 183 (1991).
4. D. Ferreday, P. J. Mitchell, G. D. Wilcox and B. Greaves, *Brit. Corros. J.* **28,** 185 (1993).
5. J. Telegdi, E. Kalman and F. H. Karman, *Corros. Sci.* **33,** 1099 (1992).
6. F. Dabosi, Y. Derbali, M. Etman, A. Shniri and A. Desavignac, *J. Appl. Electrochem.* **21,** 255 (1991).
7. J. L. Jang, Y. Li, X. R. Ye, Z. W. Wang and Q. Liu, *Corrosion (NACE)* **49,** 266 (1993).
8. Yu. I. Kuznetsov and A. F. Rashkohikov, *Zasch. Met.* **28,** 249 (1992).
9. M. Yamashita, H. Miyuki, Y. Matsuda, H. Nagano and T. Misawa, *Corros. Sci.* **36,** 283 (1994).
10. Neelam Plata, B. V. Rao, S. N. Dubey and D. M. Puri, *Ind. J. Chem.* **23A,** 397 (1984).
11. M. Jayalakshmi and V. S. Muralidharan, *Corrosion reviews* **12,** 305 (1994).
12. Ph. Refait, D. Rezel and J. M. R. Genin, *Progress in the Understanding and Prevention of Corrosion* (Edited by J. M. Costa and A. D. Mercer) Vol. 2, P1122 (1995).
13. T. Murakawa, S. Nagaura and N. Hackerman, *Corros. Sci.* **7,** 79 (1967).
14. T. Murakawa, T. Kato, S. Nagaura and N. Hackerman, *Corros. Sci.* **8,** 463 (1968).
15. N. Hackerman, E. S. Snaveley and I. S. Payne, *J. Electrochem. Soc.* **113,** 677 (1966).
16. K. Aramaki and N. Hackerman, *J. Electrochem. Soc.* **116,** 568 (1969).
17. E. D. Mor and C. Wrubi, *Brit. Corros. J.* **11,** 199 (1976).